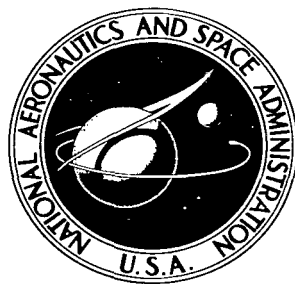


NASA TECHNICAL NOTE



NASA TN D-4248

C.1



NASA TN D-4248

LOAN COPY: RETURN TO
AFWL (WLIL-2)
KIRTLAND AFB, N MEX

USE OF SIMILARITY PARAMETERS
FOR EXAMINATION OF GEOMETRY
CHARACTERISTICS OF HIGH-EXPANSION-RATIO
AXIAL-FLOW TURBINES

by Arthur J. Glassman and Warner L. Stewart

*Lewis Research Center
Cleveland, Ohio*



USE OF SIMILARITY PARAMETERS FOR EXAMINATION OF GEOMETRY
CHARACTERISTICS OF HIGH-EXPANSION-RATIO
AXIAL-FLOW TURBINES

By Arthur J. Glassman and Warner L. Stewart

Lewis Research Center
Cleveland, Ohio

NATIONAL AERONAUTICS AND SPACE ADMINISTRATION

For sale by the Clearinghouse for Federal Scientific and Technical Information
Springfield, Virginia 22151 - CFSTI price \$3.00

USE OF SIMILARITY PARAMETERS FOR EXAMINATION OF GEOMETRY CHARACTERISTICS OF HIGH-EXPANSION-RATIO AXIAL-FLOW TURBINES

by Arthur J. Glassman and Warner L. Stewart

Lewis Research Center

SUMMARY

The use of similarity concepts as a means for examining the geometry characteristics of high-expansion-ratio axial-flow turbines is described. The similarity parameters are discussed with respect to turbine stage and overall characteristics. Interrelations among the number of stages, the stage diameter variation, the turbine expansion ratio, and the stage-similarity-parameter variation are developed and explored. To illustrate the use of the developed relations, the turbine geometry characteristics associated with several example high-expansion-ratio applications are estimated.

The highest overall efficiency in a multistage turbine is attained when the stage similarity parameters are maintained approximately constant at or near the stage optimum values. A turbine with a constant mean diameter cannot meet this requirement, especially for a high-expansion-ratio application. Appropriate proportioning of stage work and stage diameter as a function of stage-exit volume flow is used to develop relations for estimating the turbine geometry characteristics for a constant stage-parameter design.

More stages are required for the constant stage-parameter design than for the constant mean-diameter design. For the high-expansion-ratio cases, the rate of increase of stage diameter may become so severe as to exceed practical limitations. A limit imposed on the stagewise increase in diameter resulted in a reduction in the overall diameter variation but in a further increase in the number of stages. The turbine geometry characteristics obtained for a nuclear rocket, a mercury Rankine cycle, and alkali-metal Rankine cycle applications are to be considered only as estimates useful for making the parametric studies associated with system preliminary design analyses.

INTRODUCTION

One early phase of power and propulsion system design studies is usually an examination of component geometry characteristics over a range of operating conditions. Estimation techniques are usually employed for these parametric examinations rather than time-consuming detailed design procedures. For turbines, geometry characteristics can be estimated reasonably well through the use of similarity parameters, which are dimensionless groups of pertinent design variables (ref. 1). Theoretical analyses in conjunction with experimental experience have established correlations between performance and certain of the similarity parameters (refs. 2 and 3).

Reference 2 presents a method that can be used to relate the efficiency level for an axial-flow turbine to the number of stages and the blade mean diameter by means of the turbine velocity ratio, which is an aerodynamic-loading similarity parameter. This method is based on the assumption of a constant blade mean diameter and does not account for performance effects associated with the turbine channel-geometry variation, which can be severe for high-expansion-ratio applications. Reference 3 presents a concept wherein optimum channel geometry as well as optimum stage loading can be specified through the use of two of three interrelated similarity parameters: turbine velocity ratio, specific speed, and specific diameter. Specific diameter is a geometry parameter, and specific speed is a parameter that provides a link between loading and geometry.

The purposes of this report are (1) to provide a means for estimating the geometry characteristics of high-expansion-ratio axial-flow turbines, and (2) to conduct an examination of these characteristics to gain an insight into the limitations and requirements imposed by high-expansion-ratio applications. The similarity concepts presented in reference 3 are used as the basis for this study. The significance of the stage and overall similarity parameters are discussed. Interrelations among the number of stages, the stage diameter variation, the turbine expansion ratio, and the stage-similarity-parameter variation are developed and explored. To illustrate the use of the developed relations, the turbine-geometry characteristics associated with several example applications are estimated.

SIMILARITY PARAMETER CHARACTERISTICS

Similarity considerations (ref. 1) show that only four parameters are needed to describe completely the characteristics of turbomachines that handle compressible fluids. These considerations are Mach number, Reynolds number, and two other characteristic values. Parameters that contain rotative speed and rotor diameter appear to be

desirable for these other characteristic values. These parameters can be provided by the similarity concept in the form of specific speed and specific diameter (ref. 3), which are also interrelated with other frequently used turbine parameters. Mach number and Reynolds number effects are usually secondary; therefore, for preliminary design studies, where secondary effects can be ignored, specific speed and specific diameter provide the basic correlation between stage characteristics and performance. In this section, the similarity parameters of interest are presented and discussed with respect to turbine stage and overall characteristics.

Stage Parameters

Specific speed and specific diameter (ref. 3) for a turbine stage are

$$N_s = \frac{NQ^{1/2}}{H_{id}^{3/4}} \quad (1)$$

and

$$D_s = \frac{DH_{id}^{1/4}}{Q^{1/2}} \quad (2)$$

respectively. (The symbols are defined in appendix A.) With the International System of units used in this report, specific speed and specific diameter are truly dimensionless. The values for these parameters, however, are often quoted with rotative speed N in revolutions per minute, stage-exit volumetric flow Q in cubic feet per second, stage ideal work H_{id} in foot-pounds per pound, and blade mean diameter D in feet. The dimensionless values of specific speed and specific diameter used in this report can be converted to the corresponding values in these U. S. customary units by multiplying by 129 and 0.420, respectively.

Specific speed and specific diameter are interrelated with other commonly used turbine parameters. An aerodynamic loading parameter of interest is the turbine velocity ratio

$$\nu = \frac{U}{(2H_{id})^{1/2}} \quad (3)$$

Combining equations (1), (2), and (3) with

$$U = \frac{ND}{2} \quad (4)$$

yields

$$N_s D_s = 2 \sqrt{2} \nu \quad (5)$$

The specification of two of these three defined similarity parameters, therefore, also serves to specify the third.

For equation (5) to be valid, the ideal work H_{id} definitions used in equations (1) to (3) must be the same. Ideal work is based on either a total- to static-pressure ratio, as used for these parameters in reference 3, or a total- to total-pressure ratio, as used for these parameters in reference 4. Often, a basis of total- to static-pressure ratio is used for single-stage turbines, while a basis of total- to total-pressure ratio is used for the individual stages of multistage turbines. For the purposes of this report, it is not necessary to specify the definition of ideal work except to say that it is the same for all parameters discussed.

Specification of two of the three previously defined similarity parameters for a turbine stage results in the specification of a stage loading, as expressed by turbine velocity ratio, and a stage geometry. The geometry aspect for axial-flow stages can be expressed in terms of hub- to tip-radius ratio. Combining equations (1), (2), and (4) with

$$Q = AV_x = \pi D^2 \left(\frac{1-R}{1+R} \right) V_x \quad (6)$$

yields

$$N_s D_s^3 = \frac{2}{\pi} \left(\frac{U}{V_x} \right) \left(\frac{1+R}{1-R} \right) \quad (7)$$

As seen from equation (7), for any given values of N_s and D_s , the assumption of a value for the velocity diagram ratio V_x/U , which generally is within a narrow range in actual practice, serves to fix the hub- to tip-radius ratio.

Some of the interrelations just discussed are shown in figure 1, where specific diameter is plotted against specific speed. The solid lines are for constant values of turbine velocity ratio and represent the relation expressed by equation (5). The dashed

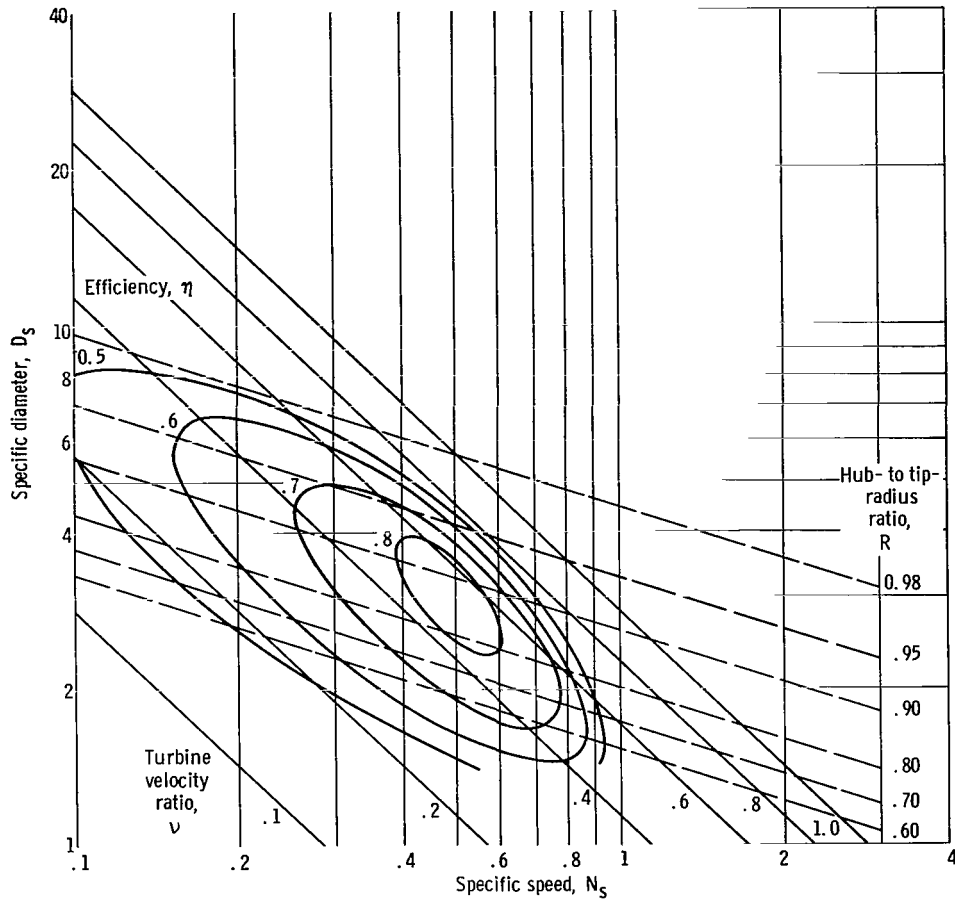


Figure 1. - Effect of specific speed and specific diameter on stage efficiency and geometry.

lines are for constant values of hub- to tip-radius ratio and represent equation (7) with a typical value of $V_x/U = 0.7$.

As mentioned previously, specific speed and specific diameter are used to provide a correlation between stage characteristics and performance. Such a correlation is developed in reference 3 for some particular cases, and an example of efficiency contours generated for an impulse stage is shown in figure 1. These contours differ from those presented in reference 3 because tip clearance was assumed to be a constant fraction of stage diameter, rather than a constant fraction of blade height as in reference 3. It can be seen that high efficiency is confined to a small area on the $N_s - D_s$ diagram. To obtain good performance from a turbine stage, therefore, values for two of the similarity parameters must be specified, and these must be selected so as to place the design point within the zone of high efficiency.

Stagewise Variation

For highest overall efficiency, the stage efficiencies must all be high, and the stage parameters, therefore, should be maintained approximately constant (at or near optimum) for all stages throughout the turbine. The ramifications of this requirement for good performance with respect to turbine geometry are explored for several cases.

Constant mean diameter. - With the mean diameter constant, equations (4) and (3) show that stage ideal work H_{id} must be constant. Equations (1) or (2), show that the stage-exit volume flow Q must be constant throughout the turbine. For a constant mean-diameter turbine to meet the requirement for constant stage parameters, therefore, flow must be incompressible. If flow is not incompressible, as in any actual case, the stage parameters cannot all be maintained constant as desired for high efficiency in all stages.

The ramifications of the foregoing conclusion for any actual case, where Q increases from the first to the last stage, are shown by maintaining each of the parameters constant in turn and examining the relative locations (as determined from eqs. (1) to (5)) of the various stage points on the $N_s - D_s$ diagram. Plotted in figure 2, which is a repeat of figure 1, are lines representing the stagewise variation in similarity parameters for the constant velocity ratio, constant specific speed, and constant specific diameter designs for a constant mean-diameter turbine. The length of each line represents the range of variations caused by an order of magnitude change in Q . The lines were arbitrarily centered within the maximum-efficiency island, but the lengths of these lines are independent of their locations.

As seen from figure 2, a turbine with a high expansion ratio, such as the order of magnitude shown, has a stage-operating-point spread that is sufficiently large to cause a significant variation among the efficiencies of the individual stages. Many of the stages could have efficiencies that are 10 to 20 points or more lower than that of the most efficient stage. A turbine with a constant mean diameter, therefore, can not provide maximum overall efficiency for a high-expansion-ratio application. On the other hand, a moderate expansion ratio, such as perhaps 2 to 3 less across the turbine, does not result in a stage-operating-point spread large enough to cause a significant degradation in the efficiency of any of the stages. In this case, a turbine with a constant mean diameter could reasonably be expected to yield good overall performance.

Variable mean diameter. - Consider again the desired condition for high overall efficiency wherein the stage parameters are maintained constant. In this case, the restriction of a constant mean diameter is not imposed. Under these conditions, equations (1) and (2) show that

$$H_{id} \propto Q^{2/3}$$

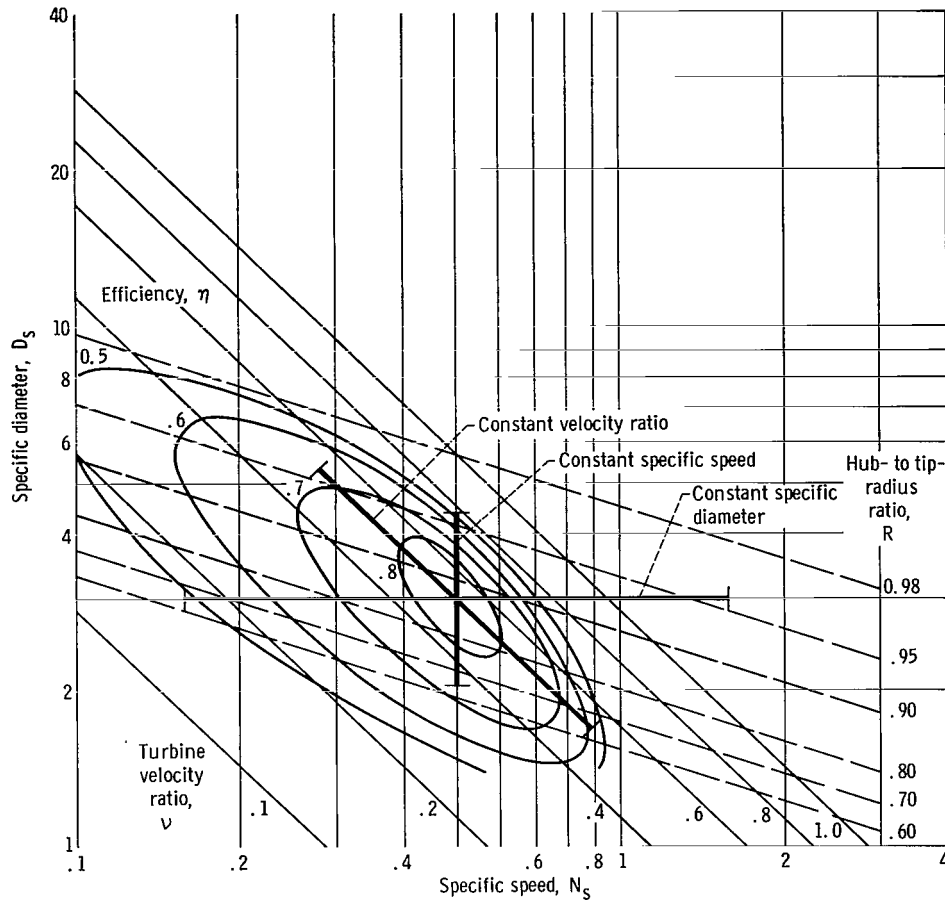


Figure 2. - Effect of volumetric flow rate variation on stage design point of constant diameter turbine. (Length of each heavy line represents effects of order of magnitude variation in volumetric flow.)

and

$$D \propto Q^{1/3}$$

It is, therefore, possible to maintain the stage parameters constant through appropriate specifications of stage work and diameter as indicated by these proportionalities. The resultant turbine will have stage work and diameter increasing from the first to the last stage.

The indicated proportionalities are used as the basis for estimating and exploring the geometry characteristics (diameter and number of stages) of high-expansion-ratio turbines. The diameter variation in the turbine must be examined, however, to ascertain whether the stage-to-stage increases remain reasonable.

Overall Parameters

The similarity parameters discussed for a single stage also can be applied on an overall turbine basis as follows:

$$\bar{N}_s = \frac{NQ_{ex}^{1/2}}{\bar{H}_{id}^{3/4}} \quad (8)$$

$$\bar{D}_s = \frac{D_{av} \bar{H}_{id}^{1/4}}{Q_{ex}^{1/2}} \quad (9)$$

$$\bar{v} = \frac{U_{av}}{(2\bar{H}_{id})^{1/2}} \quad (10)$$

The value for U_{av} is some appropriate average value such that D_{av} is obtained from equation (4). Volumetric flow at the turbine exit is used for defining these parameters.

Of these overall parameters, specific speed is the most significant because its value is almost always determined by application considerations only, while the values for specific diameter and velocity ratio depend on the nature of the evolved geometry. Further discussion and use of overall parameters in this report, therefore, are limited to overall specific speed. Overall and stage specific speeds are related by

$$\frac{\bar{N}_s}{N_s} = \left(\frac{Q_{ex}}{Q} \right)^{1/2} \left(\frac{H_{id}}{\bar{H}_{id}} \right)^{3/4} \quad (11)$$

This equation provides the link between overall and stage parameter characteristics, and it serves as a basic relation for the estimation of turbine geometry characteristics.

Equation (8) can be restated to show the considerations that contribute to the value of overall specific speed. Substituting the expression

$$Q_{ex} = wv_{ex}(1 - m) \quad (12)$$

for exit volumetric flow in equation (8) yields

$$\bar{N}_s = \frac{N[\bar{w}v_{ex}(1 - m)]^{1/2}}{\bar{H}_{id}^{3/4}} \quad (13)$$

Expressing weight flow as

$$w = \frac{\bar{P}}{\eta \bar{H}_{id}} \quad (14)$$

and making this substitution in equation (13) yield

$$\bar{N}_s = \left(\frac{1}{\eta}\right)^{1/2} \left[\frac{v_{ex}(1 - m)}{\bar{H}_{id}^{5/2}} \right]^{1/2} (N\sqrt{\bar{P}}) \quad (15)$$

Thus, the overall specific speed can be expressed as the product of three terms. The first term reflects expected performance, which can be reasonably estimated. The second term depends only on the specified fluid and thermodynamic cycle conditions. This second term is useful for evaluating the effects that different fluids (in cases where a choice is available) have on the turbine. The third term almost always is dictated by the application requirements. Often, both rotative speed and power are specified; in other cases, the product $N\sqrt{\bar{P}}$ rather than the individual values of N and \bar{P} is established by the application.

MULTISTAGE GEOMETRY CHARACTERISTICS

The previously discussed considerations are used as a basis for developing a technique for estimating and exploring the number of stages, the first- and last-stage diameters, and the stage-diameter variation for high-performance, high-expansion-ratio turbines. The constant stage-parameter case is examined first, followed by the case where stage-to-stage diameter increase (or flare) is subject to limitations.

Constant Stage-Parameter Design

Relations are first developed for estimating the number of stages and then for determining diameters and diameter variation.

Number of stages. - The hypothetical incompressible-flow case is used in the development of the estimating technique for the compressible-flow case. For the case of incompressible flow with a constant specific speed and a constant rotative speed, the stage ideal works $H_{id, inc}$, as seen from equation (1), are equal. If the relatively small turbine reheat effect is neglected, the number of stages for the incompressible-flow case is expressed as

$$\bar{n}_{inc} = \frac{\bar{H}_{id}}{H_{id, inc}} \quad (16)$$

For this case, $Q = Q_{inc} = Q_{ex}$ and $N_s = N_{s, inc}$. Substituting equation (16) into equation (11) then yields

$$\frac{\bar{N}_s}{N_{s, inc}} = \frac{1}{\bar{n}_{inc}^{3/4}}$$

or

$$\bar{n}_{inc} = \left(\frac{N_{s, inc}}{\bar{N}_s} \right)^{4/3} \quad (17)$$

With \bar{N}_s known from the application and $N_{s, inc}$ set at some desired value, \bar{n}_{inc} is obtained from equation (17). This value is used subsequently for the determination of \bar{n} .

Volumetric flow increases from the first to the last stage in the actual case. In the similarity parameter equations, the value of Q refers to the flow at the exit of each stage; the change in Q , consequently, is stepwise rather than continuous through the turbine. This change is indicated by the steps in figure 3, where stage-exit volumetric flow is plotted against the summation of ideal work from inlet to exit. For this analysis, a continuous variation in Q is assumed, as indicated by the curve in figure 3. The effect of this assumption is relatively minor, especially where more than a few stages are involved, and it becomes more negligible with an increasing number of stages.

Referring to figure 3, consider a small interval of ideal work ΔH_{id} , as indicated. Let the increment in the number of stages associated with this interval be Δn for the compressible-flow case. Within this small interval, the actual flow is considered incompressible, and the values of Q and H_{id} , therefore, are considered constant. The incremental ideal work is expressed as

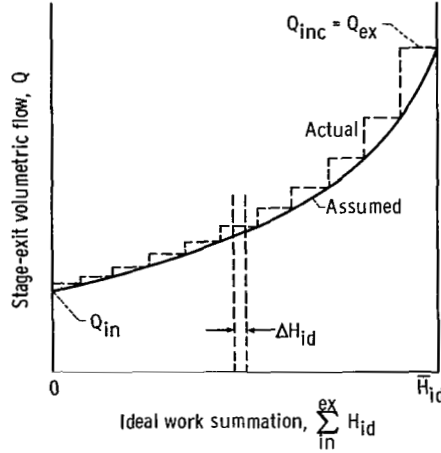


Figure 3. - Variation in stage-exit volumetric flow with ideal work expended.

$$\Delta H_{id} = \Delta n H_{id} \quad (18)$$

Substituting equation (18) into equation (1) yields

$$N_s = \frac{NQ^{1/2}}{\left(\frac{\Delta H_{id}}{\Delta n}\right)^{3/4}} \quad (19)$$

Since Q_{inc} and $H_{id, inc}$, as shown previously, are constant, equation (1) when written for the incompressible-flow case can be combined with equation (16) to yield

$$N_{s, inc} = \frac{NQ_{inc}^{1/2}}{\left(\frac{\bar{H}_{id}}{\bar{n}_{inc}}\right)^{3/4}} \quad (20)$$

which is valid for the small interval being considered.

Combining equations (19) and (20) and setting Q_{inc} equal to Q_{ex} yield

$$\Delta n = \bar{n}_{inc} \left(\frac{Q_{ex}}{Q}\right)^{2/3} \left(\frac{N_s}{N_{s, inc}}\right)^{4/3} \left(\frac{\Delta H_{id}}{\bar{H}_{id}}\right) \quad (21)$$

Since the specific speed for this case is maintained constant throughout the turbine, N_s can be set to equal to $N_{s, inc}$, and equation (21) reduces to

$$\Delta n = \bar{n}_{inc} \left(\frac{Q_{ex}}{Q} \right)^{2/3} \left(\frac{\Delta H_{id}}{\bar{H}_{id}} \right) \quad (22)$$

Integrating equation (22) from the inlet to the exit yields

$$\frac{\bar{n}}{\bar{n}_{inc}} = \int_0^1 \left(\frac{Q_{ex}}{Q} \right)^{2/3} d \left(\frac{\Sigma H_{id}}{\bar{H}_{id}} \right) \quad (23)$$

The value of the integral in equation (23) can be determined for the case of an ideal gas, where Q is analytically related to ΣH_{id} . A relation between the stage ratio \bar{n}/\bar{n}_{inc} and the volumetric expansion ratio Q_{ex}/Q_{in} is developed in appendix B and shown in figure 4 for values of the specific-heat ratio of 1.2, 1.4, and 1.67. It might be noted that the three curves are not extended to the same value of the expansion ratio because for any given pressure ratio across the turbine, the volumetric expansion ratio decreases with an increasing specific-heat ratio. For any given value of Q_{ex}/Q_{in} , the

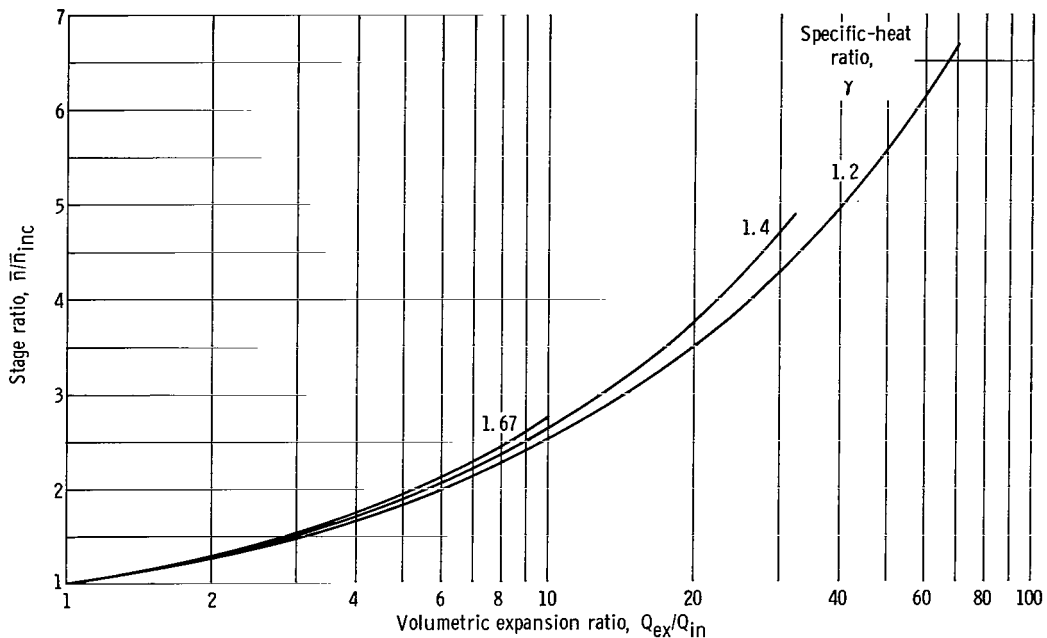


Figure 4. - Effect of volumetric expansion ratio on number of stages for constant stage-parameter turbine.

value of \bar{n}/\bar{n}_{inc} is nearly independent of the specific-heat ratio; in addition, although not obvious from the equations, this relation appears to be completely independent of turbine efficiency. Figure 4 shows that the relative increase in the required number of stages attributable to the increase in volumetric flow through the turbine is quite significant, especially at the higher expansion ratios.

The relation shown in figure 4 was derived specifically for a perfect gas. For certain other cases, the ideal gas law is approximately valid, and the isentropic expansion path is approximated quite well by an equation of the form $pv^n = \text{constant}$ (as shown in ref. 5 for a condensing metal vapor). Figure 4, therefore, should be at least approximately applicable for such cases. It is shown subsequently by means of numerical examples that, for the case of condensing metal vapors, the ideal gas values of \bar{n}/\bar{n}_{inc} obtained from figure 4 are very close to those obtained from a numerical integration of equation (23) that uses Mollier chart properties and accounts for the loss in volumetric flow caused by condensation.

Diameter. - With the similarity parameters specified constant, the diameters of the first and last stages can be estimated readily. Rotative speed N is known from the application and, after the estimation of a turbine efficiency, so are the inlet and exit volumetric flows. Combining equations (1) and (2) to eliminate last-stage ideal work yields the equation for the last-stage or exit diameter

$$D_{ex} = D_s \left(\frac{Q_{ex} N_s}{N} \right)^{1/3} \quad (24)$$

Since the similarity parameter values for the first stage are the same as those for the last stage, the first-stage or inlet diameter can be estimated as

$$D_{in} = D_{ex} \left(\frac{Q_{in}}{Q_{ex}} \right)^{1/3} \quad (25)$$

It can be seen from equation (25) that there can be a significant increase in diameter between the first and last stages; for expansion ratios of 10 or greater, for example, the last-stage diameter is more than twice that of the first stage. The manner in which this variation in diameter takes place within the turbine requires examination. An analytical procedure for determining the diameter variation is developed in appendix B. The ratio of the stage diameter to the inlet diameter as a function of the stage fraction (stage number divided by total number of stages) is plotted in figure 5 for several expansion ratios. The turbine flare (increase in stage diameter with stage number)

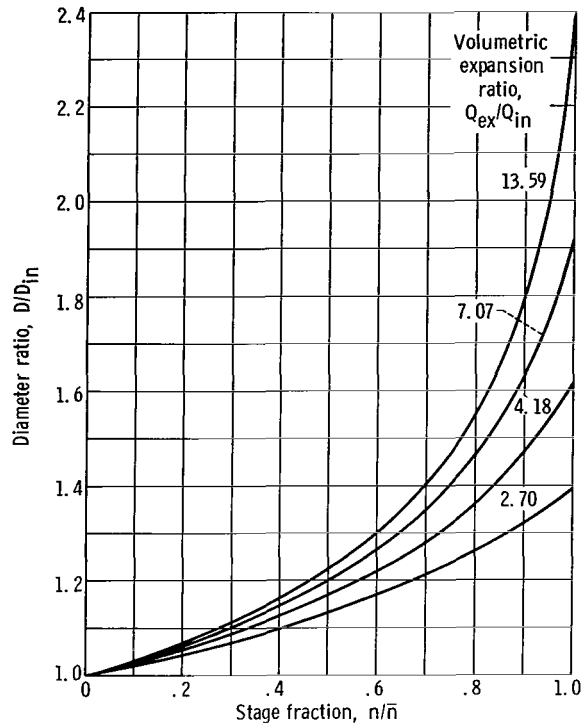


Figure 5. - Effect of volumetric expansion ratio on diameter variation for constant stage-parameter turbine. Specific-heat ratio, 1.4; efficiency, 0.75.

increases from inlet to exit, with the increase becoming more severe at the higher expansion ratios. In fact, the indicated flares at the exit ends of high-expansion-ratio turbines are so severe that they undoubtedly exceed practical limitations with respect to expecting the flow to follow such a path efficiently.

The use of a constant stage-parameter design for high-expansion-ratio turbines, therefore, appears to be limited by the required end-wall flare near the exit. Modification of the design philosophy to eliminate the flare problem and the effect of this modification on the turbine geometry are discussed in the next section.

Flare-Limited Design

A flare-limited design is defined as one in which the stage similarity parameters are all maintained constant from the inlet to the point where a specified flare is reached, and thereafter the flare and only one of the similarity parameters, the velocity ratio, are maintained constant to the exit. This modification will affect the number of stages and the specific speeds of the flare-limited stages as well as the stage diameters.

Number of stages. - A flare-limited design as compared with a constant stage-

parameter design requires an increased number of stages because of the reduced diameter, and consequently reduced work, of the flare-limited stages. Since stage specific speed is not constant throughout the turbine, the overall stage ratio is obtained by integration of equation (21) rather than of equation (22):

$$\frac{\bar{n}}{\bar{n}_{inc}} = \int_0^1 \left(\frac{Q_{ex}}{Q} \right)^{2/3} \left(\frac{N_s}{N_{s, inc}} \right)^{4/3} d \left(\frac{\Sigma H_{id}}{\bar{H}_{id}} \right) \quad (26)$$

The analytical procedure for evaluating equation (26) for an ideal gas is presented in appendix C. The relation between the stage ratio and the volumetric expansion ratio is shown in figure 6 for a specific-heat ratio of 1.4 and for several values of the limiting flare, represented by the flare-limit parameter $dD/Dd(n/\bar{n}_{inc})$. As was indicated by figure 4, the effect of the specific-heat ratio on this relation is quite small. The smallest flare-limit parameter shown in figure 6 is 0.1; this value corresponds to an increase in diameter of 10 percent per stage if $\bar{n}_{inc} = 1$. Smaller limiting values of the flare parameter are not of interest, since stagewise flare is inversely proportional to \bar{n}_{inc} , which in most cases for high-expansion-ratio applications will be quite a bit larger

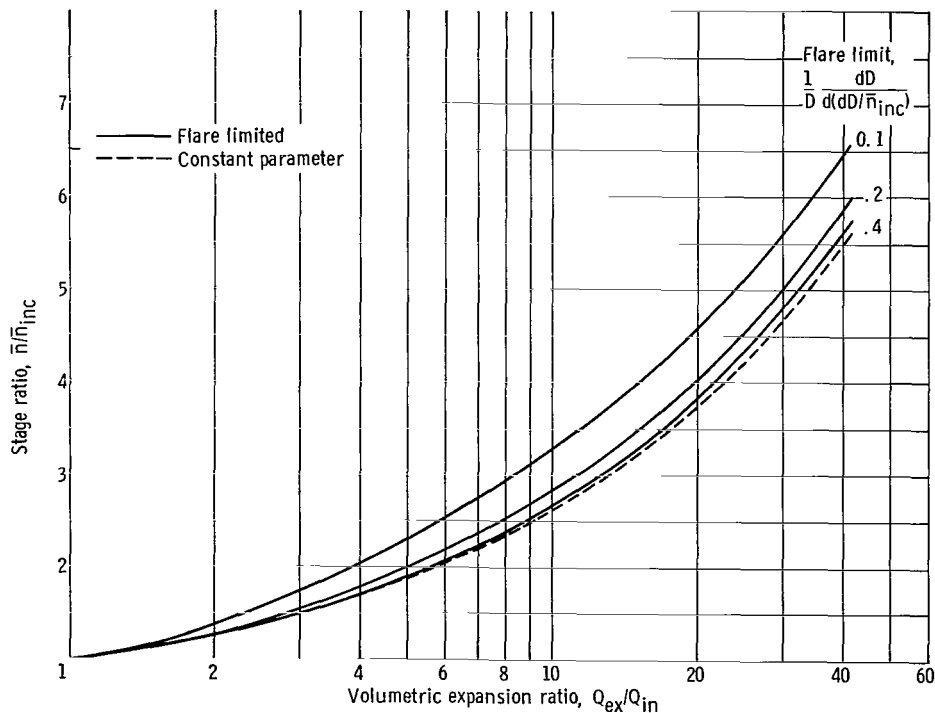


Figure 6. - Effect of volumetric expansion ratio and flare limit on number of stages. Specific heat ratio, 1.4.

than 1. The effect of a flare limit on the number of stages is rather small, about 5 percent or less, when the flare-limit parameter is 0.2 or greater, values that should apply to most cases of interest.

Diameter. - The analytical procedure used to determine the diameter variation for a flare-limited turbine is presented in appendix C. The effect of the flare limit on the diameter variation is illustrated in figure 7, where the ratio of the stage diameter to the inlet diameter is plotted against stage fraction (stage number divided by number of stages for the constant parameter case) for two expansion ratios, each with several flare limits. As seen from figure 7, a decrease in the limiting flare causes a decrease in the diameter variation through the turbine and, as was also shown previously, an increase in the number of stages.

The specification of a flare limit causes the specific speeds of the flare-limited stages to vary and, thus there will be some effect on stage performance. The specific speed variation through the turbine is estimated from equations (C6) and (C10) in appendix C. For an expansion ratio of 10, for example, the ratio of last-stage to first-stage specific speeds is 1.93, 1.50, and 1.20 for flare-limit parameter values of 0.1, 0.2, and 0.4, respectively. This variation is not nearly so severe as that in a constant-diameter turbine where the comparable ratio of specific speeds would be about 3.16. The effect of the specific speed variation on stage performance, therefore, would be

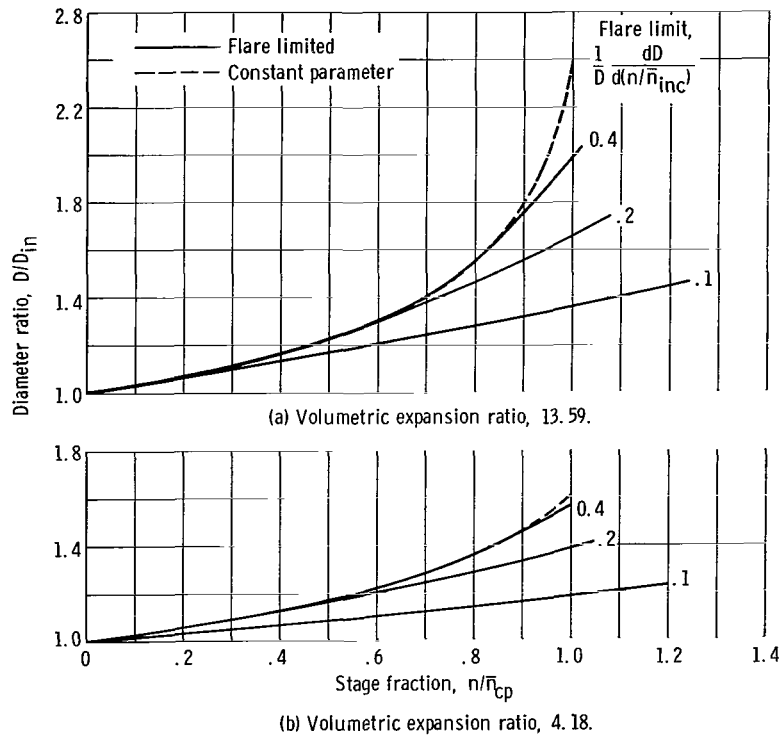


Figure 7. - Effect of flare limit on diameter variation. Specific heat ratio, 1.4; efficiency, 0.75.

considerably less than that indicated in figure 2 for the constant-diameter constant-velocity-ratio turbine.

GEOMETRY CHARACTERISTICS FOR EXAMPLE APPLICATIONS

The turbine-geometry-estimation techniques used to examine the general characteristics of high-expansion-ratio turbines were applied to several example applications, and the results are presented in this section. The requirements analyzed are for (1) a nuclear rocket pump-drive turbine, (2) a mercury Rankine cycle power turbine, and (3) alkali-metal Rankine-cycle power turbines.

Assumptions and Procedure

The stage similarity parameters were assumed constant for the three example applications. The values assumed were a specific speed N_s of 0.465 and a velocity ratio ν of 0.40. The corresponding specific diameter is 2.43. Experience has shown that these assumed parameter values are consistent with relatively high efficiency. If performance is compromised, then values are selected that will result in fewer stages than the number calculated herein. An overall efficiency of 0.75 was assumed for the nuclear rocket gas turbine, and the thermodynamic calculations were made with the use of the ideal gas equations and values of 1.4 for the specific-heat ratio and 4124 joules per kilogram per $^{\circ}\text{K}$ for the gas constant. For the Rankine cycle vapor turbines, where condensation occurs, an overall efficiency of 0.70 was assumed, and the properties of reference 6 along with the associated Mollier diagrams were used for the thermodynamic calculations.

From the turbine requirements and the fluid properties, the ideal work \bar{H}_{id} and the exit volume flow Q_{ex} are calculated. Substitution of these calculated values, along with the specified rotative speed N , into equation (8) yields the overall specific speed \bar{N}_s . With the use of the selected stage specific speed N_s , a value for the number of stages \bar{n}_{inc} for the incompressible-flow case is obtained from equation (17). With the volumetric ratio Q_{ex}/Q_{in} known, the overall stage ratio \bar{n}/\bar{n}_{inc} for an ideal gas is obtained from figure 4 and that for condensing vapor is obtained from equation (23) by numerical integration with the use of the thermodynamic data. As will be shown subsequently, if an average value of the specific-heat ratio for a condensing vapor expansion is used, figure 4 can be used for a condensing vapor as well as for an ideal gas. With \bar{n}/\bar{n}_{inc} determined, the number of stages \bar{n} is known.

With the specified values for the stage specific speed N_s , the velocity ratio ν , and

the specific diameter D_s , the exit diameter D_{ex} is calculated from equation (24). Equation (25) yields the inlet diameter D_{in} . The geometry characteristics determined in this manner are only estimates. These characteristics can be very useful for preliminary parametric analyses but should not be used as design values for any given turbine.

Results

The requirements for each example application and the pertinent results are now presented.

Nuclear rocket. - Typical nuclear rocket pump-drive requirements, obtained from reference 7, are listed in the following table with the pertinent calculated parameters and the estimated geometry characteristics.

Fluid	Hydrogen
Turbine-inlet temperature, T_{in} , $^{\circ}\text{K}$	1032
Turbine-inlet pressure, p_{in} , N/m^2	6.89×10^6
Turbine pressure ratio, p_{in}/p_{ex}	12.68
Rotative speed N , rad/sec	5010
Shaft power, \bar{P} , W	8.77×10^6
Ideal work, \bar{H}_{id} , J/kg	7.71×10^6
Exit volume flow, Q_{ex} , m^3/sec	7.28
Overall specific speed, \bar{N}_s	0.0929
Incompressible-flow number of stages, \bar{n}_{inc}	8.57
Volume ratio, Q_{ex}/Q_{in}	7.76
Stage ratio, \bar{n}/\bar{n}_{inc}	2.31
Number of stages \bar{n}	19.8
Exit diameter, D_{ex} , m	0.214
Inlet diameter, D_{in} , m	0.108

For the nuclear-rocket turbine, the constant stage-parameter design for the assumed parameter values would require about 20 stages.

It might be noted that a constant mean-diameter turbine with a constant stage velocity ratio would require the same number of stages as that calculated for the incompressible-flow case with the same stage velocity ratio. The number of stages required for the incompressible-flow case is about nine, which agrees well with the eight-stage constant mean-diameter turbine evolved in reference 7. The diameters for the constant stage-parameter turbines are small, 0.108 meter at the inlet and 0.214 meter

TABLE I. - MERCURY RANKINE-CYCLE

TURBINE CHARACTERISTICS

Parameter	Rotative speed, N rad/sec	
	1257	2513
Turbine-inlet temperature, T_{in} , °K	950	950
Turbine-inlet pressure, p_{in} , N/m ²	1.82×10^6	1.82×10^6
Turbine-exit pressure, p_{ex} , N/m ²	9.64×10^4	9.64×10^4
Shaft power, \bar{P} , W	6.3×10^4	6.3×10^4
Ideal work, \bar{H}_{id} , J/kg	8.36×10^4	8.36×10^4
Exit volume flow, Q_{ex} , m ³ /sec	0.270	0.270
Overall specific speed, \bar{N}_s	0.133	0.266
Incompressible-flow number of stages, \bar{n}_{inc}	5.34	2.12
Volume ratio, Q_{ex}/Q_{in}	11.63	11.63
Stage ratio, \bar{n}/\bar{n}_{inc}	2.90	2.90
Number of stages, \bar{n}	15.5	6.2
Exit diameter, D_{ex} , m	0.1129	0.0895
Inlet diameter, D_{in} , m	0.0498	0.0395

at the exit. With the high value of \bar{n}_{inc} , there should be no concern about any flare limitation.

Mercury Rankine cycle. - For the mercury Rankine-cycle power system application, two rotative speeds are considered. The first is 1257 radians per second, which corresponds to the design speed for the SNAP-8 system (presented in ref. 8), and the second is 2513 radians per second, a value corresponding to twice the design speed. The turbine requirements are given in table I with the pertinent calculated parameters and the estimated geometry characteristics.

At the lower rotative speed, about five stages are required for the incompressible-flow case. (The ref. 8 design, which has a constant mean diameter and a constant stage velocity ratio, uses four stages.) About 16 stages are required for a constant stage-parameter design. The diameters are quite small, ranging from 0.0498 meter at the inlet to 0.1129 meter at the exit. Doubling the rotative speed results in the number of stages being reduced by about 60 percent and the diameter being reduced by about 20 percent. At the lower rotative speed, the value of \bar{n}_{inc} is sufficiently large that flare limitations should not affect the geometry characteristics; at the higher rotative speed, however, flare limitations would probably necessitate a small increase in the number of stages and a small decrease in the exit diameter.

The value of \bar{n}/\bar{n}_{inc} equal to 2.90 (table I) was obtained from a numerical integration of equation (23) with the use of Mollier chart equilibrium properties and a loss in

volume flow due to condensation. An average specific-heat ratio for this expansion, determined by $p_{in} v_{in}^{\gamma_{av}} = p_{ex} v_{ex}^{\gamma_{av}}$, is $\gamma_{av} = 1.2$. With this specific-heat ratio, a value of \bar{n}/\bar{n}_{inc} equal to 2.72 is obtained from figure 4, which was derived on the basis of ideal gas flow. The agreement between the two values of \bar{n}/\bar{n}_{inc} is good.

Alkali-metal Rankine cycle. - Turbine characteristics for the alkali-metal Rankine-cycle systems were determined for the working fluids sodium, potassium, rubidium, and cesium over a range of rotative speeds. The vapors are assumed to be saturated at the turbine inlet. The turbine requirements are presented in table II with pertinent calculated parameters and the estimated geometry characteristics. Since rotative speed is a variable, some of the values presented in table II are normalized as indicated.

TABLE II. - ALKALI-METAL RANKINE-CYCLE TURBINE CHARACTERISTICS

[Turbine-inlet temperature, 1389° K; turbine temperature ratio, 0.75; shaft power, 3.3×10^5 W.]

Fluid	Ideal work, \bar{H}_{id} , J/kg	Exit volume flow, Q_{ex} , m ³ /sec	Overall specific speed, N_s/N , sec/rad	Incompressible flow number of stages, $\bar{n}_{inc} N^{4/3}$, (rad/sec) ^{4/3}	Volume ratio, Q_{ex}/Q_{in}	Stage ratio, \bar{n}/\bar{n}_{inc}	Number of stages, $\bar{n} N^{4/3}$, (rad/sec) ^{4/3}	Exit diameter, $D_{ex} N^{1/3}$, m(rad/sec) ^{1/3}	Diameter ratio, D_{ex}/D_{in}
Sodium	9.86×10^5	4.64	0.761×10^{-4}	11.17×10^4	12.6	2.84	31.7×10^4	3.15	2.32
Potassium	5.03	1.55	.732	11.80	7.16	2.22	26.2	2.19	1.927
Rubidium	2.04	1.08	1.200	6.07	5.76	1.97	11.95	1.94	1.791
Cesium	1.23	.964	1.650	3.96	4.91	1.85	7.33	1.87	1.700

The number of stages and the last-stage diameters for the four fluids are plotted against rotative speed in figure 8. At the lower rotative speeds, the number of stages required for a constant stage-parameter design becomes quite large, while at the higher rotative speeds, except for sodium, the diameters become rather small. The ratio of exit to inlet diameter is about 2 for all fluids. The effect of fluid on the geometry characteristics reflects primarily the higher volume flow and expansion ratio associated with a decrease in fluid molecular weight.

In table III, the values of \bar{n}/\bar{n}_{inc} obtained from numerical integration of equation (23) with the use of the equilibrium properties are compared with the values obtained from figure 4 with the use of an average value of 1.2 (ref. 5) for the specific-heat ratio.

The comparison in table III for the alkali metals and the comparison previously presented for mercury show very good agreement between the two values of \bar{n}/\bar{n}_{inc} . Therefore, the ideal gas values can be applied to condensing-vapor systems when an average value of the specific-heat ratio for the expansion process is used.

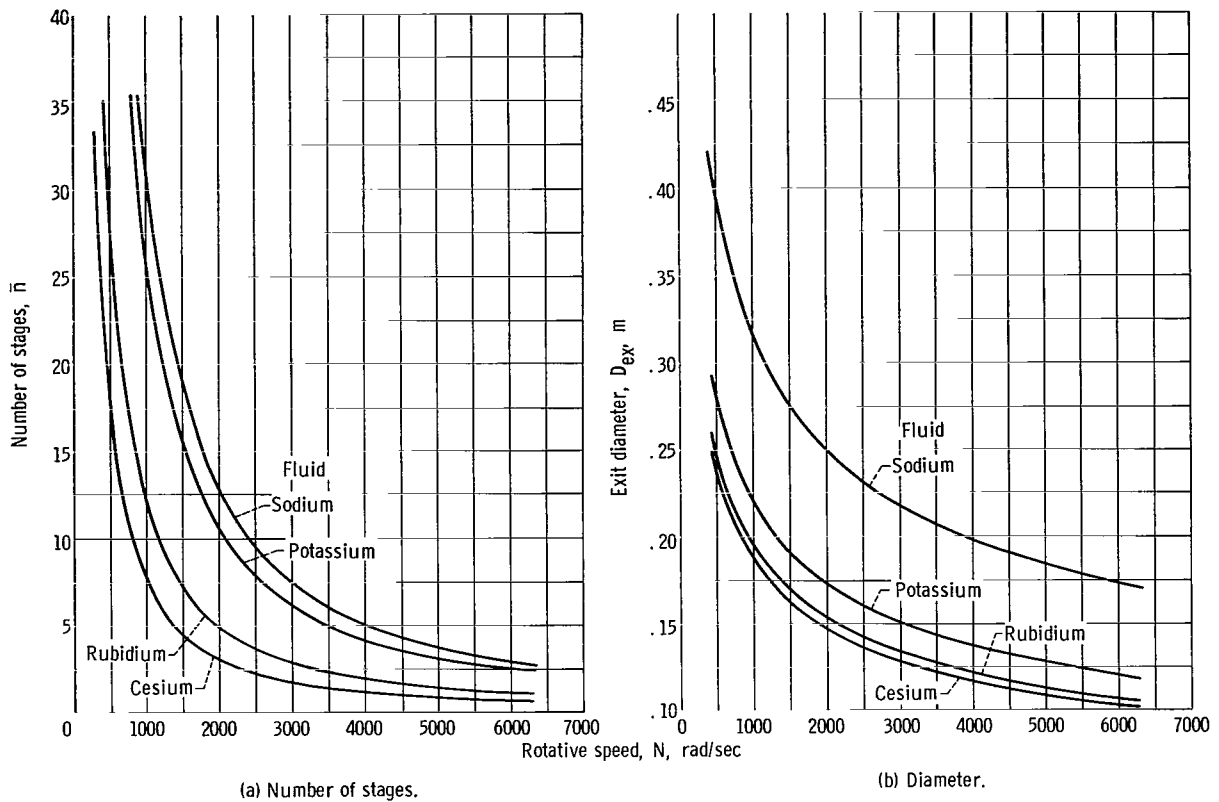


Figure 8. - Alkali-metal Rankine-cycle turbine characteristics.

TABLE III. - COMPARISON OF
STAGE RATIO VALUES

Fluid	Stage ratio, \bar{n}/\bar{n}_{inc}	
	Equation (23)	Figure 4
Sodium	2.84	2.82
Potassium	2.22	2.15
Rubidium	1.97	1.95
Cesium	1.85	1.82

CONCLUDING REMARKS

The use of similarity concepts as a means for examining the geometry characteristics of high-expansion-ratio axial-flow turbines is presented. The similarity parameters are discussed with respect to turbine stage and overall characteristics. Interrelations among the geometry characteristics, the similarity parameters, and the turbine expansion ratio are developed and explored. To illustrate the use of the developed relations, the turbine geometry characteristics associated with several example applications are estimated.

The highest overall efficiency in a multistage turbine is attained when the stage similarity parameters are maintained approximately constant at or near the stage optimum values. The stage similarity parameters, however, cannot be maintained constant in a turbine with a constant mean diameter. For a high volumetric expansion-ratio application, the stagewise variation in stage parameter values is large enough to cause a significant degradation in the efficiencies of some of the stages. A turbine with a constant mean diameter, therefore, cannot provide maximum overall efficiency for a high-expansion-ratio application.

The stage similarity parameters can be maintained constant by appropriate proportioning of the stage work and the stage diameter as a function of stage-exit volume flow. With these proportionalities as a basis, a technique was developed for estimating the turbine stage number and diameter variation characteristics. The constant stage-parameter design requires more stages than a constant mean-diameter design, with the proportion increasing at higher expansion ratios. The diameter increases from the inlet to the exit, with the rate of increase becoming larger toward the exit. For high-expansion-ratio turbines, the rate of the diameter increase may become so severe as to exceed practical limitations.

A design modification examined for the purpose of eliminating any severe increase in diameter involved imposing a limitation on the stagewise increase. This modification resulted in a reduction in the overall diameter variation in the turbine but an increase in the number of stages. In addition, the similarity parameters associated with the diameter-limited stages could not all be maintained constant; this variation, however, was much less severe than that for a constant mean-diameter turbine.

Lewis Research Center,
National Aeronautics and Space Administration,
Cleveland, Ohio, August 1, 1967,
120-27-04-66-22.

APPENDIX A

SYMBOLS

A	annulus area, m^2	V_x	axial component of gas velocity, m/sec
c_p	heat capacity at constant pressure, $\text{J}/(\text{kg})(^\circ\text{K})$	v	specific volume, m^3/kg
D	mean diameter, m	w	mass flow, kg/sec
D_s	specific diameter	x	$\gamma/(\gamma - 1)$
$F(y)$	$(1 - \eta y)/(1 - y)^x$	y	$\Sigma H_{id}/c_p T_{in}$
H_{id}	specific ideal work, J/kg	γ	specific-heat ratio
K	constant value of limiting flare	η	efficiency
m	turbine-exit moisture fraction	ν	turbine velocity ratio
N	rotative speed, rad/sec	Subscripts:	
N_s	specific speed	av	average
n	number of stages	cp	constant parameter
P	power, W	ex	turbine exit
p	absolute pressure, N/m^2	in	turbine inlet
Q	stage-exit volumetric flow, m^3/sec	inc	incompressible flow case
R	ratio of hub radius to tip radius	Superscripts:	
T	absolute temperature, $^\circ\text{K}$	—	overall
U	blade speed, m/sec	*	position of limiting flare

APPENDIX B

DETERMINATION OF GEOMETRY CHARACTERISTICS FOR CONSTANT STAGE-PARAMETER TURBINE

With the assumption that the turbine characteristics can be treated as continuously varying quantities, the stage ratio and the diameter variation through the turbine are readily evaluated for the case of an ideal gas.

Stage Ratio

Integrating equation (22) from the inlet to any general point in the turbine yields the general stage-ratio expression for a constant stage-parameter turbine:

$$\frac{n}{\bar{n}_{inc}} = \int_0^{\Sigma H_{id}/\bar{H}_{id}} \left(\frac{Q_{ex}}{Q} \right)^{2/3} d \left(\frac{\Sigma H_{id}}{\bar{H}_{id}} \right) \quad (B1)$$

To evaluate this expression, consider an expansion from some inlet state p_{in}, T_{in} to any given state p, T ; for this expansion, the volume ratio is

$$\frac{Q}{Q_{in}} = \frac{v}{v_{in}} = \left(\frac{T}{T_{in}} \right) \left(\frac{p_{in}}{p} \right) \quad (B2)$$

and the ideal work is

$$\Sigma H_{id} = c_p T_{in} \left[1 - \left(\frac{p}{p_{in}} \right)^{(\gamma-1)/\gamma} \right] = \frac{c_p T_{in}}{\eta} \left(1 - \frac{T}{T_{in}} \right) \quad (B3)$$

From equation (B3),

$$\frac{T}{T_{in}} = 1 - \eta \frac{\Sigma H_{id}}{c_p T_{in}} \quad (B4)$$

and

$$\frac{p}{p_{in}} = \left(1 - \frac{\Sigma H_{id}}{c_p T_{in}}\right)^{\gamma/(\gamma-1)} \quad (B5)$$

Substituting equations (B4) and (B5) into equation (B2), and letting $x = \gamma/(\gamma - 1)$ and $y = \Sigma H_{id}/c_p T_{in}$, for purposes of brevity, yield

$$\frac{Q}{Q_{in}} = \frac{1 - \eta y}{(1 - y)^x} \quad (B6)$$

Again for purposes of brevity, the functional notation $F(y)$ is introduced such that

$$F(y) = \frac{Q}{Q_{in}} = \frac{1 - \eta y}{(1 - y)^x} \quad (B6a)$$

For the exit state p_{ex}, T_{ex} , where $\Sigma H_{id} = \bar{H}_{id}$, equation (B6) becomes

$$\frac{Q_{ex}}{Q_{in}} = \frac{1 - \eta \bar{y}}{(1 - \bar{y})^x} = F(\bar{y}) \quad (B7)$$

Dividing equation (B7) by equation (B6a) yields

$$\frac{Q_{ex}}{Q} = \frac{F(\bar{y})}{F(y)} \quad (B8)$$

Substituting equation (B8) into equation (B1) and noting that $\Sigma H_{id}/\bar{H}_{id} = y/\bar{y}$ yield

$$\frac{n}{\bar{n}_{inc}} = \frac{[F(\bar{y})]^{2/3}}{\bar{y}} \int_0^y \frac{dy}{[F(y)]^{2/3}} \quad (B9)$$

The integral in equation (B9) is evaluated by means of the prismoidal formula

$$\int_0^y \frac{dy}{[F(y)]^{2/3}} = \frac{y}{6} \left\{ 1 + 4 \left[F\left(\frac{y}{2}\right) \right]^{-2/3} + [F(y)]^{-2/3} \right\} \quad (B10)$$

Combining equations (B9) and (B10) yields

$$\frac{n}{\bar{n}_{inc}} = \frac{y[F(\bar{y})]^{2/3}}{6\bar{y}} \left\{ 1 + 4 \left[F\left(\frac{y}{2}\right) \right]^{-2/3} + [F(y)]^{-2/3} \right\} \quad (B11)$$

This general stage ratio expression represents the number of stages required from the inlet to any point in the turbine corresponding to y . This ratio is used subsequently for the determination of the diameter variation.

An expression for the overall stage ratio, required to evaluate equation (23), is obtained by setting y equal to \bar{y} in equation (B11). This yields, after simplification,

$$\frac{\bar{n}}{\bar{n}_{inc}} = \frac{1}{6} \left\{ [F(\bar{y})]^{2/3} + 4 \left[\frac{F(\bar{y})}{F\left(\frac{\bar{y}}{2}\right)} \right]^{2/3} + 1 \right\} \quad (B12)$$

Equations (B12) and (B7) provide a means for relating \bar{n}/\bar{n}_{inc} to Q_{ex}/Q_{in} for the case of a perfect gas in a constant stage-parameter turbine. This relation is presented in figure 4 and discussed in the body of the report.

Diameter Variation

Differentiating equations (4), (3), and (1) yields

$$\frac{dD}{D} = \frac{dU}{U} \quad (B13)$$

$$\frac{dU}{U} = \frac{1}{2} \frac{dH_{id}}{H_{id}} \quad (B14)$$

and

$$\frac{dH_{id}}{H_{id}} = \frac{2}{3} \frac{dQ}{Q} \quad (B15)$$

which combine to give

$$\frac{dD}{D} = \frac{1}{3} \frac{dQ}{Q} \quad (B16)$$

Integrating from the inlet to any point corresponding to y yields

$$\frac{D}{D_{in}} = [F(y)]^{1/3} \quad (B17)$$

Equations (B17) and (B11), therefore, provide a means for relating diameter variation to stage number. This relation is presented in figure 5 and discussed in the body of the report. The values of the volumetric expansion ratio shown in figure 5 correspond to values of \bar{y} of 0.3, 0.4, 0.5, and 0.6.

The stagewise fractional increase in diameter (or flare) dD/D_{dn} is of interest for determining the point in the turbine where limiting values are initially encountered. The logarithms of the terms in equation (B6a) are differentiated

$$\frac{dQ}{Q} = \left[\frac{F'(y)}{F(y)} \right] dy = \left(\frac{x}{1-y} - \frac{\eta}{1-\eta y} \right) dy \quad (B18)$$

and substituted into equation (B16) to yield

$$\frac{dD}{D} = \frac{1}{3} \left[\frac{F'(y)}{F(y)} \right] dy \quad (B19)$$

In differential form, equation (B9) is

$$d\left(\frac{n}{\bar{n}_{inc}}\right) = \frac{1}{\bar{y}} \left[\frac{F(\bar{y})}{F(y)} \right]^{2/3} dy \quad (B20)$$

Dividing equation (B19) by equation (B20) yields the relation for evaluating pointwise flare:

$$\frac{1}{D} \frac{dD}{d\left(\frac{n}{\bar{n}_{inc}}\right)} = \frac{\bar{y}}{3} \left[\frac{F'(y)}{F(y)} \right] \left[\frac{F(y)}{F(\bar{y})} \right]^{2/3} \quad (B21)$$

Equation (B21) is used subsequently for examining flare-limited turbines.

APPENDIX C

DETERMINATION OF GEOMETRY CHARACTERISTICS FOR FLARE-LIMITED TURBINE

The geometry characteristics of the flare-limited turbine differ from those of the constant stage-parameter turbine as a result of the imposed diameter limitations. The analytical procedure for examining the affected characteristics is presented in this appendix.

Stage Ratio

Since specific speed N_s is constant and equal to $N_{s, inc}$ from the inlet to the point of initial flare limitation, equation (26) can be rewritten as

$$\frac{\bar{n}}{\bar{n}_{inc}} = \int_0^{\Sigma H_{id}^* / \bar{H}_{id}} \left(\frac{Q_{ex}}{Q} \right)^{2/3} d \left(\frac{\Sigma H_{id}}{\bar{H}_{id}} \right) + \int_{\Sigma H_{id}^* / \bar{H}_{id}}^1 \left(\frac{Q_{ex}}{Q} \right)^{2/3} \left(\frac{N_s}{N_s^*} \right)^{4/3} d \left(\frac{\Sigma H_{id}}{\bar{H}_{id}} \right) \quad (C1)$$

where the $*$ values refer to the initial point of flare limitation. The first term on the right side of equation (C1) is evaluated by means of equation (B11)

$$\frac{n^*}{\bar{n}_{inc}} = \frac{y^* [F(\bar{y})]^{2/3}}{6\bar{y}} \left\{ 1 + 4 \left[F \left(\frac{y^*}{2} \right) \right]^{-2/3} + [F(y^*)]^{-2/3} \right\} \quad (C2)$$

provided that the value of y^* is known. With a prespecified value of limiting flare K , y^* is obtained by an iterative solution of equation (B21) such that

$$K = \left[\frac{1}{D} \frac{dD}{d\left(\frac{n}{\bar{n}_{\text{inc}}}\right)} \right]^* = \frac{\bar{y}}{3} \left[\frac{F'(y^*)}{F(y^*)} \right] \left[\frac{F(y^*)}{F(\bar{y})} \right]^{2/3} \quad (\text{C3})$$

To evaluate the second term on the right side of equation (C1), equation (C1) is written

$$\frac{\bar{n}}{\bar{n}_{\text{inc}}} - \frac{n^*}{\bar{n}_{\text{inc}}} = \int_{n^*/\bar{n}_{\text{inc}}}^{\bar{n}/\bar{n}_{\text{inc}}} d\left(\frac{n}{\bar{n}_{\text{inc}}}\right) = \int_{y^*/\bar{y}}^1 \left[\frac{F(\bar{y})}{F(y)} \right]^{2/3} \left(\frac{N_s}{N_s^*} \right)^{4/3} d\left(\frac{y}{\bar{y}}\right) \quad (\text{C4})$$

Using the specific speed definition yields

$$N = \frac{N_s^* H_{\text{id}}^{3/4}}{Q^{1/2}} = \frac{N_s H_{\text{id}}^{3/4}}{Q^{1/2}} \quad (\text{C5})$$

and

$$\left(\frac{N_s}{N_s^*} \right)^{4/3} = \left[\frac{F(y)}{F(y^*)} \right]^{2/3} \left(\frac{H_{\text{id}}^*}{H_{\text{id}}} \right) \quad (\text{C6})$$

From equations (B13) and (B14),

$$\frac{dH_{\text{id}}}{H_{\text{id}}} = 2 \frac{dD}{D} \quad (\text{C7})$$

and for the constant flare region,

$$\frac{dD}{D} = K d\left(\frac{n}{\bar{n}_{\text{inc}}}\right) \quad (\text{C8})$$

Thus,

$$\frac{dH_{id}}{H_{id}} = 2K d\left(\frac{n}{\bar{n}_{inc}}\right) \quad (C9)$$

and integrating into the constant flare region to any point yields

$$\frac{H_{id}^*}{H_{id}} = \exp\left[-2K\left(\frac{n}{\bar{n}_{inc}} - \frac{n^*}{\bar{n}_{inc}}\right)\right] \quad (C10)$$

Combining equations (C10) and (C6) with the differential form of equation (C4) and reimposing the limits of integration yield

$$\int_{n^*/\bar{n}_{inc}}^{\bar{n}/\bar{n}_{inc}} \exp\left[2K\left(\frac{n}{\bar{n}_{inc}} - \frac{n^*}{\bar{n}_{inc}}\right)\right] d\left(\frac{n}{\bar{n}_{inc}}\right) = \left[\frac{F(\bar{y})}{F(y^*)}\right]^{2/3} \int_{y^*/\bar{y}}^1 d\left(\frac{y}{\bar{y}}\right) \quad (C11)$$

Performing the indicated integration results in

$$\frac{\bar{n}}{\bar{n}_{inc}} = \frac{n^*}{\bar{n}_{inc}} + \frac{1}{2K} \ln\left\{1 + 2K\left[\frac{F(\bar{y})}{F(y^*)}\right]^{2/3} \left(1 - \frac{y^*}{\bar{y}}\right)\right\} \quad (C12)$$

where the value of n^*/\bar{n}_{inc} is obtained from equation (C2). The effect of the flare limitation on the overall stage ratio is shown in figure 6.

Diameter Variation

The diameter variation from the inlet to the initial point of flare limitation is expressed by equation (B17); that is,

$$\frac{D}{D_{in}} = [F(y)]^{1/3} \quad \text{for } 0 \leq y \leq y^* \quad (C13)$$

For the constant-flare region, integration of equation (C8) yields

$$\frac{D}{D^*} = \exp \left[K \left(\frac{n}{\bar{n}_{\text{inc}}} - \frac{n^*}{\bar{n}_{\text{inc}}} \right) \right] \quad (\text{C14})$$

Since

$$\frac{D}{D_{\text{in}}} = \left(\frac{D^*}{D_{\text{in}}} \right) \left(\frac{D}{D^*} \right) \quad (\text{C15})$$

the following equation is obtained for the constant-flare region:

$$\frac{D}{D_{\text{in}}} = [F(y^*)]^{1/3} \exp \left[K \left(\frac{n}{\bar{n}_{\text{inc}}} - \frac{n^*}{\bar{n}_{\text{inc}}} \right) \right] \quad \text{for } y^* \leq y \leq \bar{y} \quad (\text{C16})$$

The effect of the flare limitation on the diameter variation is presented in figure 7.

REFERENCES

1. Shepherd, D. G.: Principles of Turbomachinery. The Macmillan Co. 1956.
2. Stewart, Warner L.: A Study of Axial-Flow Turbine Efficiency Characteristics in Terms of Velocity Diagram Parameters. Paper No. 61-WA-37, ASME, 1961.
3. Baljé, O. E.: A Study on Design Criteria and Matching of Turbomachines: Part A - Similarity Relations and Design Criteria of Turbines. J. Eng. Power, vol. 84, no. 1, Jan. 1962, pp. 83-102.
4. Wood, Homer J.: Current Technology of Radial-Inflow Turbines for Compressible Fluids. J. Eng. Power, vol. 85, no. 1, Jan. 1963, pp. 72-83.
5. Goldman, Louis J.: Expansion and Flow Characteristics of Initially Saturated Sodium, Potassium, and Cesium Vapors. NASA TN D-3743, 1966.
6. Meisl, C. J.; and Shapiro, A.: Thermodynamic Properties of Alkali Metal Vapors and Mercury. Rep. No. R60FPD358-A, General Electric Co., Nov. 9, 1960.
7. Rohlik, Harold E.: Investigation of Eight-Stage Bleed-Type Turbine for Hydrogen-Propelled Nuclear Rocket Applications. I - Design of Turbine and Experimental Performance of First Two Stages. NASA TM X-475, 1961.
8. Slone, Henry O.: SNAP-8 Development Status. Space Power Systems Advanced Technology Conference. NASA SP-131, 1966, pp. 147-168.

"The aeronautical and space activities of the United States shall be conducted so as to contribute . . . to the expansion of human knowledge of phenomena in the atmosphere and space. The Administration shall provide for the widest practicable and appropriate dissemination of information concerning its activities and the results thereof."

—NATIONAL AERONAUTICS AND SPACE ACT OF 1958

NASA SCIENTIFIC AND TECHNICAL PUBLICATIONS

TECHNICAL REPORTS: Scientific and technical information considered important, complete, and a lasting contribution to existing knowledge.

TECHNICAL NOTES: Information less broad in scope but nevertheless of importance as a contribution to existing knowledge.

TECHNICAL MEMORANDUMS: Information receiving limited distribution because of preliminary data, security classification, or other reasons.

CONTRACTOR REPORTS: Scientific and technical information generated under a NASA contract or grant and considered an important contribution to existing knowledge.

TECHNICAL TRANSLATIONS: Information published in a foreign language considered to merit NASA distribution in English.

SPECIAL PUBLICATIONS: Information derived from or of value to NASA activities. Publications include conference proceedings, monographs, data compilations, handbooks, sourcebooks, and special bibliographies.

TECHNOLOGY UTILIZATION PUBLICATIONS: Information on technology used by NASA that may be of particular interest in commercial and other non-aerospace applications. Publications include Tech Briefs, Technology Utilization Reports and Notes, and Technology Surveys.

Details on the availability of these publications may be obtained from:

SCIENTIFIC AND TECHNICAL INFORMATION DIVISION
NATIONAL AERONAUTICS AND SPACE ADMINISTRATION
Washington, D.C. 20546